

See discussions, stats, and author profiles for this publication at: <https://www.researchgate.net/publication/6951488>

Comparison of Model Chemistry and Density Functional Theory Thermochemical Predictions with Experiment for Formation of Ionic Clusters of the Ammonium Cation Complexed with Water a...

ARTICLE *in* THE JOURNAL OF PHYSICAL CHEMISTRY A · JULY 2005

Impact Factor: 2.69 · DOI: 10.1021/jp0514372 · Source: PubMed

CITATIONS

33

READS

136

3 AUTHORS, INCLUDING:



Frank Pickard

National Heart, Lung, and Blood Institute

16 PUBLICATIONS 284 CITATIONS

SEE PROFILE



George C Shields

Bucknell University

96 PUBLICATIONS 3,976 CITATIONS

SEE PROFILE

Comparison of Model Chemistry and Density Functional Theory Thermochemical Predictions with Experiment for Formation of Ionic Clusters of the Ammonium Cation Complexed with Water and Ammonia; Atmospheric Implications

Frank C. Pickard IV, Meghan E. Dunn, and George C. Shields*

Contribution from the Department of Chemistry, Hamilton College, 198 College Hill Road, Clinton, New York 13323

Received: March 18, 2005; In Final Form: April 5, 2005

The G2, G3, CBS-QB3, and CBS-APNO model chemistry methods and the B3LYP, B3P86, mPW1PW, and PBE1PBE density functional theory (DFT) methods have been used to calculate ΔH° and ΔG° values for ionic clusters of the ammonium ion complexed with water and ammonia. Results for the clusters NH_4^+ -(NH_3) $_n$ and $\text{NH}_4^+(\text{H}_2\text{O})_n$, where $n = 1-4$, are reported in this paper and compared against experimental values. Agreement with the experimental values for ΔH° and ΔG° for formation of $\text{NH}_4^+(\text{NH}_3)_n$ clusters is excellent. Comparison between experiment and theory for formation of the $\text{NH}_4^+(\text{H}_2\text{O})_n$ clusters is quite good considering the uncertainty in the experimental values. The four DFT methods yield excellent agreement with experiment and the model chemistry methods when the aug-cc-pVTZ basis set is used for energetic calculations and the 6-31G* basis set is used for geometries and frequencies. On the basis of these results, we predict that all ions in the lower troposphere will be saturated with at least one complete first hydration shell of water molecules.

Introduction

The Gaussian- n (G_n)^{1,2} and complete basis set (CBS)³⁻⁵ model chemistries have been developed in an attempt to accurately calculate changes in enthalpy and free energy for gas-phase reactions. To achieve chemical accuracy, computed values of ΔG must be correct to within 1 kcal/mol. A serious challenge to these methods is accurate calculation of the energetics of formation of ionic clusters. Calculation of the enthalpy and free energy changes of ionic clusters is difficult, as the basis set superposition error (BSSE) and fragment relaxation energies for these complexes have large effects.⁶ In principle, the Gaussian- n and complete basis set model chemistries,¹⁻⁵ which extrapolate the energies to the complete basis set limit, should provide energies that do not need to be corrected for limitations in the basis set used for the different geometries in an ionic cluster calculation. To better evaluate the ability of the Gaussian and complete basis set model chemistries¹⁻⁵ to accurately model gas-phase ionic cluster formation, we have measured their performance against 15 reactions in the NIST database.⁷ We have recently tested a variety of density functional theory (DFT) functionals for their ability to accurately reproduce deprotonation reactions,⁸ as compared against a NIST dataset of highly accurate values and against model chemistry methods.⁹ We have used the best of these functionals to examine their ability to model the structure and energetics of the ammonium ion clusters. In this paper, we report on our test of the performance of the G2, G3, CBS-QB3, and CBS-APNO methods and the B3LYP, B3P86, mPW1PW, and PBE1PBE density-functionals against this dataset. Using data from an agricultural site in the state of North Carolina, we discuss the atmospheric implications of our results.

Methods

The G_n and CBS methods are model chemistries developed with the goal of obtaining highly accurate values for thermo-

chemical parameters.^{1-5,10-22} In the CBS models, a series of calculations are made on a defined geometry, and a complete basis set model chemistry includes corrections for basis set truncation errors. The G_n model chemistries, which were the first systematic model chemistries to be developed with broad applicability to a wide range of chemical problems, have a similar philosophy and implementation.²³ The G2 and G3 methods fall between the two CBS methods in terms of computational cost. The details of the basis sets and formulas used to obtain the final energies can be found in the original publications and a recent text.^{1-5,23} These methods have been used to calculate accurate values for enthalpies of formation, atomization energies, ionization potentials, electron affinities, proton affinities, isodesmic reactions, cation-atom reactions, molecule-atom reactions, deprotonation reactions, accurate thermodynamic cycles for pK_a calculations, hydrogen bonding of neutral water clusters, and hydrogen bonding of water clusters to the H_3O^+ and OH^- ions and to explore activation energy barriers and potential intermediates in chemical reactions.^{9,12-22,24-31}

We used the G2,¹ G3,² CBS-QB3,³ and CBS-APNO^{4,5} methods and the B3LYP,^{32,33} B3P86,^{32,34} mPW1PW,³⁵ and PBE1PBE³⁶ density functionals implemented within Gaussian 03, version B.02.³⁷ On the basis of our experience with gas-phase deprotonation reactions,⁸ we have used the DFT functionals to optimize each structure at the DFT/6-31G* level. Single-point energy calculations at the DFT/aug-cc-pVTZ level were then used with the frequency output at the DFT/6-31G* level to obtain ΔH° and ΔG° values for each reaction. No corrections were made for basis set superposition error. The absence of imaginary frequencies verified that all structures were true minima at their respective levels of theory. The geometries of all the stationary points and absolute energies in hartrees of each stationary point at each level of theory are available as Supporting Information. All values reported in this paper are for a standard state of 1 atm.

TABLE 1: Energetics for the Successive Addition of Ammonia to Ammonium Ion Clusters for the Model Chemistries CBS-QB3, CBS-APNO, G3, and G2 and the DFT Methods B3LYP, B3P86, mPW1PW, and PBE1PBE^a

$$\text{NH}_4^+(\text{NH}_3)_{n-1} + \text{NH}_3 \rightarrow \text{NH}_4^+(\text{NH}_3)_n$$

<i>n</i>	model chemistries				DFT methods (DFT/6-31G*)				(DFT/aug-cc-pVTZ//DFT/6-31G*)				experiment	
	QB3	APNO	G3	G2	B3LYP	B3P86	mPW1PW	PBE1PBE	B3LYP	B3P86	mPW1PW	PBE1PBE	ref 50	ref 51
ΔE_0 (kcal/mol)														
1	-26.01	-26.47	-26.12	-25.84	-33.49	-34.55	-33.85	-34.53	-26.93	-28.55	-27.94	-28.53		
2	-19.72	-19.76	-19.66	-19.46	-24.11	-24.41	-24.24	-24.75	-18.99	-19.56	-19.30	-19.73		
3	-16.14	-16.16	-16.13	-15.95	-19.32	-19.53	-19.44	-19.91	-15.07	-15.51	-15.32	-15.74		
4	-13.51	-13.52	-13.55	-13.39	-15.65	-15.74	-15.73	-16.17	-12.26	-12.51	-12.41	-12.78		
ΔH° (kcal/mol)														
1	-25.73	-25.11	-24.73	-24.45	-33.23	-35.27	-33.77	-34.52	-26.67	-29.27	-27.86	-28.52	-25.4	-24.8
2	-17.45	-17.93	-17.88	-17.68	-21.70	-22.37	-22.95	-23.40	-16.58	-17.52	-18.00	-18.39	-17.3	-15.7
3	-14.21	-14.37	-14.38	-14.20	-17.34	-16.37	-16.28	-17.94	-13.10	-12.35	-12.16	-13.77	-14.2	-13.8
4	-11.72	-11.80	-11.87	-11.70	-16.20	-14.49	-14.50	-13.74	-12.81	-11.27	-11.17	-10.35	-11.8	-12.5
σ	0.22	0.41	0.53	0.60	6.05	6.71	6.15	6.79	1.21	2.50	1.92	2.10	0.00	1.09
σ	1.26	1.40	1.36	1.27	6.67	7.41	6.91	7.58	1.27	3.00	2.52	2.93	1.09	0.00
ΔG° (kcal/mol)														
1	-18.56	-18.41	-18.09	-17.81	-25.48	-25.58	-25.91	-27.22	-18.92	-19.58	-20.00	-21.22	-18.2	-17.1
2	-9.97	-11.84	-11.60	-11.39	-13.39	-12.69	-11.48	-11.37	-8.27	-7.84	-6.54	-6.35	-10.2	-8.9
3	-7.67	-7.39	-7.08	-6.90	-9.05	-12.39	-11.88	-10.00	-4.81	-8.37	-7.76	-5.83	-6.7	-6.1
4	-3.86	-6.40	-6.98	-6.66	-2.35	-4.75	-5.59	-7.91	1.04	-1.53	-2.26	-4.53	-3.7	-3.7
σ	0.65	1.87	2.07	1.85	4.89	5.64	5.56	6.12	3.18	2.25	2.58	2.91	0.00	1.02
σ	1.39	2.53	2.57	2.31	5.81	6.51	6.36	6.87	3.07	2.39	2.50	2.84	1.02	0.00

^a Changes in energies including zero-point energies, standard state enthalpies, and standard state free energies are given for each method and compared to experimental data. Standard deviations from each experiment are given for enthalpies and free energies.

TABLE 2: Energetics for the Successive Addition of Water to Ammonium Ion Clusters for the Model Chemistries CBS-QB3, CBS-APNO, G3, and G2 and the DFT Methods B3LYP, B3P86, mPW1PW, and PBE1PBE^a

$$\text{NH}_4^+(\text{H}_2\text{O})_{n-1} + \text{H}_2\text{O} \rightarrow \text{NH}_4^+(\text{H}_2\text{O})_n$$

<i>n</i>	model chemistries				DFT methods (DFT/6-31G*)				DFT/aug-cc-pVTZ//DFT/6-31G*				experiment	
	QB3	APNO	G3	G2	B3LYP	B3P86	mPW1PW	PBE1PBE	B3LYP	B3P86	mPW1PW	PBE1PBE	ref 52	ref 51
ΔE_0 (kcal/mol)														
1	-20.30	-20.67	-20.48	-20.28	-25.31	-25.60	-25.17	-25.70	-20.52	-21.19	-20.78	-21.26		
2	-17.24	-17.24	-17.28	-17.04	-20.84	-20.91	-20.69	-21.17	-16.57	-16.93	-16.69	-17.13		
3	-14.89	-14.77	-14.94	-14.71	-17.57	-17.53	-17.42	-17.83	-13.79	-13.97	-13.89	-14.43		
4	-13.03	-12.72	-13.04	-12.72	-14.83	-14.70	-14.69	-15.14	-11.64	-11.75	-11.64	-11.95		
ΔH° (kcal/mol)														
1	-19.19	-19.28	-19.11	-18.91	-24.79	-25.16	-24.12	-25.23	-19.99	-20.74	-19.72	-20.80	-20.6	-17.3
2	-15.71	-15.70	-15.77	-15.54	-18.69	-18.80	-19.17	-19.06	-14.42	-14.82	-15.16	-15.02	-17.4	-14.7
3	-13.27	-13.20	-13.41	-13.18	-15.91	-15.89	-15.80	-16.27	-12.13	-12.33	-12.26	-12.87	-13.7	-13.4
4	-11.45	-11.18	-11.53	-11.22	-13.20	-13.08	-13.09	-13.47	-10.00	-10.13	-10.04	-10.28		-12.2
σ	1.58	1.56	1.57	1.82	3.47	3.71	3.15	3.93	2.42	2.07	1.98	1.79	0.00	3.02
σ	1.31	1.41	1.28	1.20	5.14	5.34	4.93	5.53	2.14	2.40	2.00	2.33	3.02	0.00
ΔG° (kcal/mol)														
1	-13.13	-14.03	-14.31	-14.11	-17.69	-18.08	-18.99	-18.19	-12.90	-13.66	-14.59	-13.76	-13.3	-11.4
2	-9.16	-9.26	-8.87	-8.63	-12.56	-12.59	-11.28	-12.91	-8.30	-8.61	-7.28	-8.87	-8.9	-8.2
3	-5.91	-5.52	-6.20	-5.97	-8.61	-8.04	-8.30	-9.03	-4.83	-4.48	-4.77	-5.63	-6.3	-5.9
4	-6.31	-5.77	-5.43	-5.11	-6.32	-6.32	-6.67	-6.85	-3.13	-3.37	-3.63	-3.66		-4.1
σ	0.36	0.82	0.74	0.66	4.39	4.47	4.61	4.90	1.15	1.34	1.83	0.59	0.00	1.42
σ	1.73	1.92	1.89	1.68	4.86	4.95	5.15	5.35	1.19	1.61	2.03	1.43	1.42	0.00

^a Changes in energies including zero-point energies, enthalpies, and free energies are given for each method and compared to experimental data. Standard deviations from each experiment are given for enthalpies and free energies.

Results

Table 1 includes calculated values for ΔE_0 , ΔH° , and ΔG° for reactions of the ammonium cation with successive additions of ammonia, and Table 2 contains calculated values for reactions of the ammonium cation with successive additions of water. Each table also contains the experimental values from the NIST database,⁷ and the standard deviations from experiment. Table 3 shows the predicted concentrations of the different ammonium cation clusters in an agricultural area. Figure 1 shows the computed structures for $\text{NH}_4^+(\text{NH}_3)_n$, and Figure 2 displays the structures for $\text{NH}_4^+(\text{H}_2\text{O})_n$, where $n = 1-4$. The figures show the values for key atom–atom separation distances and bond

angles, for the QCISD/6-311G(d,p) structure computed with the CBS-APNO model chemistry, along with results from the PBE1PBE functional. The NH_4^+ structure has near- T_d symmetry, the $\text{NH}_4^+(\text{NH}_3)$ structure has near- C_{3v} symmetry, the $\text{NH}_4^+(\text{NH}_3)_2$ structure has near- C_{2v} symmetry, the $\text{NH}_4^+(\text{NH}_3)_3$ structure has near- C_{3v} symmetry, and the $\text{NH}_4^+(\text{NH}_3)_4$ structure has near- T_d symmetry, in agreement with previous results.^{38–41} The $\text{NH}_4^+(\text{NH}_3)_4$ structure has been observed in an inorganic crystal structure, where the crystal packing results in a roughly tetrahedral symmetry.⁴² For the $\text{NH}_4^+(\text{H}_2\text{O})_n$ clusters, previous supersonic jet expansion experiments and calculations have revealed that because of the strong hydrogen bonding ability

TABLE 3: Free Energies in kcal/mol, Equilibrium Constants, Molarity, and Number of Ammonium Ion Clusters per Cubic Centimeter Predicted To Be Present in the Atmosphere at an Agricultural Site on a Humid Day^a

reaction	ΔG°	K_c	M	N
$\text{NH}_4^+ + \text{NH}_3 \rightarrow \text{NH}_4^+(\text{NH}_3)$	-18.09	4.45×10^{14}	4.63×10^{-11}	3×10^{10}
$\text{NH}_4^+ + \text{H}_2\text{O} \rightarrow \text{NH}_4^+(\text{H}_2\text{O})$	-14.31	7.5×10^{11}	3.09×10^{-15}	2×10^6
$\text{NH}_4^+(\text{H}_2\text{O}) + \text{H}_2\text{O} \rightarrow \text{NH}_4^+(\text{H}_2\text{O})_2$	-8.869	7.8×10^7	2.80×10^{-13}	2×10^8
$\text{NH}_4^+(\text{H}_2\text{O})_2 + \text{H}_2\text{O} \rightarrow \text{NH}_4^+(\text{H}_2\text{O})_3$	-6.203	8.6×10^5	1.02×10^{-12}	6×10^8
$\text{NH}_4^+(\text{H}_2\text{O})_3 + \text{H}_2\text{O} \rightarrow \text{NH}_4^+(\text{H}_2\text{O})_4$	-5.429	2.3×10^5	3.11×10^{-10}	2×10^{11}

^a The product ion clusters and their concentrations are in boldface type.

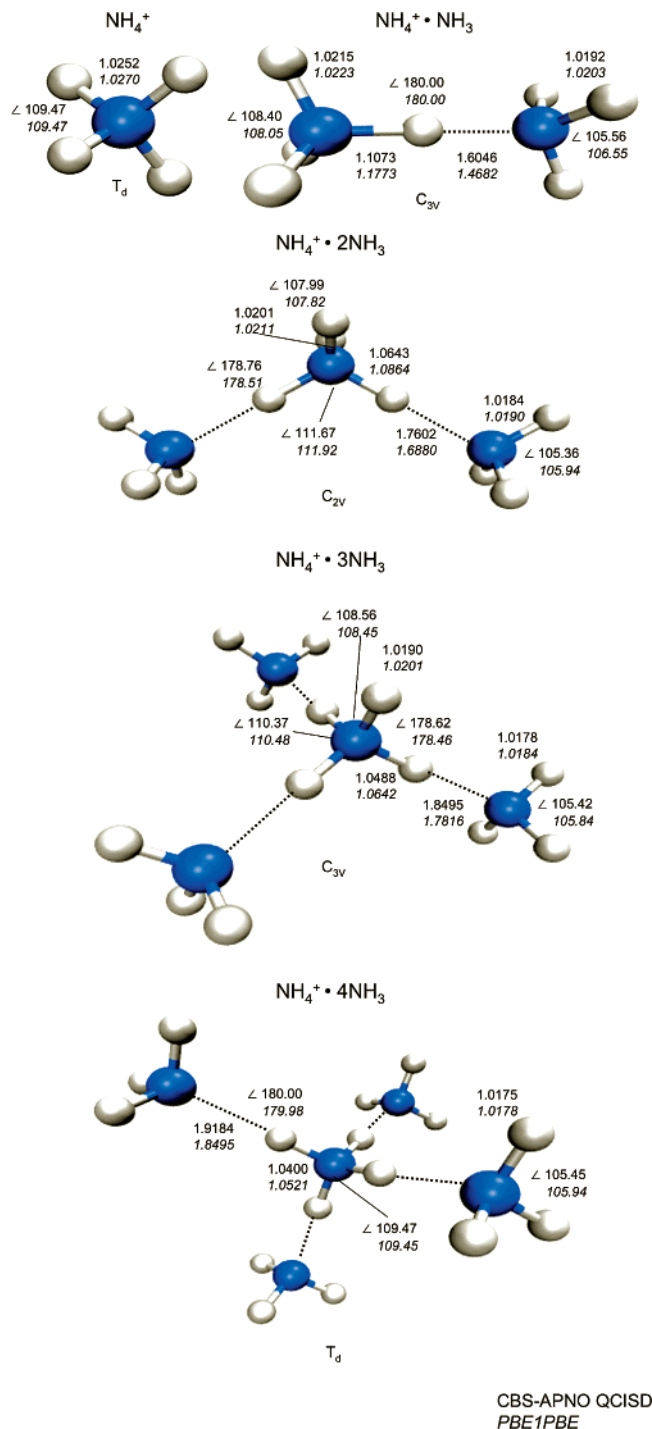


Figure 1. CBS-APNO QCISD and PBE1PBE (italics) structures of NH_4^+ , and $\text{NH}_4^+(\text{NH}_3)_n$ clusters, $n = 1-4$, with approximate symmetry labeled.

of water, structural isomers occur for these clusters starting at $n = 4$.⁴³⁻⁴⁶ Figure 2 shows that the $\text{NH}_4^+(\text{H}_2\text{O})$ structure has near- C_s symmetry, the $\text{NH}_4^+(\text{H}_2\text{O})_2$ structure has near- C_1

symmetry, the $\text{NH}_4^+(\text{H}_2\text{O})_3$ structure has near- C_3 symmetry, and the $\text{NH}_4^+(\text{H}_2\text{O})_4$ structure has near- T_d symmetry. Four supplementary files contain the G2, G3, CBS-QB3, CBS-APNO, B3LYP, B3P86, mPW1PW, and PBE1PBE energy values for each molecule and cluster reported in this paper, as well as all the geometries computed with these methods (see Supporting Information).

Discussion

Structure. The G_n and CBS methods yield similar structures, as do the density functional methods. The G2 and G3 structures are identical MP2(full)/6-31G(d) geometries, the CBS-QB3 structure is a B3LYP/CBSB7 geometry, whereas the CBS-APNO structure is determined at the QCISD/6-311G(d,p) level. For instance, the NH_4^+ structure has bond distances of 1.029, 1.028, 1.026, and 1.027 Å for the B3LYP, B3P86, mPW1PW, and PBE1PBE optimizations using the 6-31G* dataset. The MP2(full)/6-31G(d) geometry has a bond distance of 1.029 Å, the B3LYP/CBSB7 geometry has a bond distance of 1.026 Å, and the QCISD/6-311G(d,p) geometry has a bond distance of 1.025 Å. The corresponding bond angles are 109.471° for all four functionals and all four model chemistries. The near- T_d $\text{NH}_4^+(\text{NH}_3)_4$ structure has DFT N-H bond distances ranging from 1.051 to 1.054 Å on the central NH_4^+ cation and from 1.017 to 1.020 Å on the four NH_3 ligands. The hydrogen bond distances range from 1.849 to 1.859 Å and hydrogen bond angles encompass $179.98-179.99^\circ$. The H-N-H bond angles are all nearly 109.47° for the NH_4^+ cation and decrease to $105.81-105.96^\circ$ for the NH_3 ligands. For the model chemistries the MP2, B3LYP, and QCISD geometries have N-H bond distances of 1.046, 1.047, and 1.040 Å about the central NH_4^+ cation, and N-H bond distances of 1.019, 1.017, and 1.017 Å about the NH_3 ligands. The hydrogen bond distances are 1.913, 1.904, and 1.918 Å, and the hydrogen bond angles are 180.00 , 179.98 , and 180.00° for the MP2, B3LYP, and QCISD geometries used for the energy calculations in the model chemistry methods. Comparison of the $\text{NH}_4^+(\text{NH}_3)_n$ clusters reveals no significant changes in the basic geometry. These structures are similar to the global minima determined by other workers using correlated optimizations.^{39-41,47,48}

The $\text{NH}_4^+(\text{H}_2\text{O})_n$ clusters show similar agreement between methods. With the $\text{NH}_4^+(\text{H}_2\text{O})_4$ structure as an example, the N-H bond distances range from 1.038 to 1.041 Å for the DFT methods, whereas the O-H bond distances range from 0.965 to 0.969 Å. The H-O-H bond angles range from 105.18 to 105.40° , the H-N-H angles range from 109.25 to 109.30° , and the hydrogen bond angles range from 175.24 to 175.93° . The DFT hydrogen bonds for the near- T_d structure range from 1.772 to 1.796 Å, which are $0.072-0.083$ Å shorter than the hydrogen bonds in the $\text{NH}_4^+(\text{NH}_3)_n$ clusters. The MP2, B3LYP, and QCISD geometries from the model chemistry clusters also have shorter hydrogen bonds between the ammonium cation and the water ligands, with distances of 1.828, 1.796, and 1.818 Å, respectively. These hydrogen bond distances are 0.085, 0.108, and 0.100 Å shorter than the hydrogen bonds in the $\text{NH}_4^+(\text{NH}_3)_n$

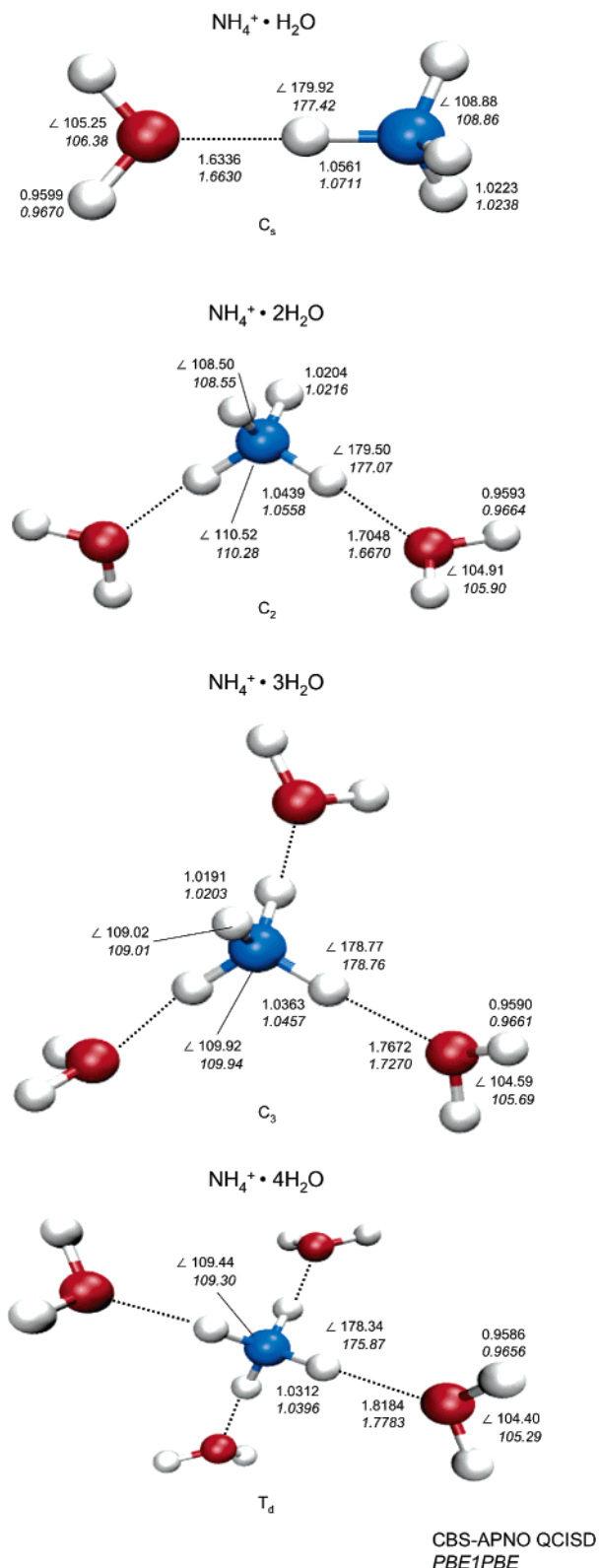


Figure 2. CBS-APNO QCISD and PBE1PBE (italics) structures of $\text{NH}_4^+(\text{H}_2\text{O})_n$ clusters, $n = 1-4$, with approximate symmetry labeled.

cluster for the MP2, B3LYP, and QCISD geometries used in the G2/G3, CBS-QB3, and CBS-APNO energy calculations. The agreement between previous calculations of ammonium-water clusters using correlated methods is excellent.^{39,43-46,49}

Thermochemistry. Examining the energetics for these reactions in Table 1, increasing the basis set size from 6-31G* to aug-cc-pVTZ for the DFT methods makes a dramatic improve-

ment in the observed energies relative to the model chemistry values. Single-point calculations using the triple- ζ basis set increases the energy of reaction by roughly 3–7 kcal/mol and brings the DFT calculations into agreement with the model chemistry results. The standard deviations of the DFT values from the two experiments decrease from 6.05–7.58 to 1.21–3.00 kcal/mol for enthalpies and from 4.89–6.87 to 2.25–3.18 for free energies. We note that the model chemistries cannot be corrected for BSSE and, in principle, do not need this correction; we have not corrected the DFT methods for BSSE. Wang and co-workers have shown that the values for ΔE become more positive as the basis set is enlarged for B3LYP calculations, and that correction for BSSE also makes the ΔE values more positive.⁴¹ For the calculated first hydration energy of NH_4^+NH_3 , they obtain a B3LYP/6-311++G**/B3LYP/6-31+G* value of -26.88 kcal/mol for ΔE_0 , which changes to -25.87 kcal/mol upon correction for BSSE.⁴¹ The uncorrected result is in excellent agreement with our DFT results and both results are within the range of model chemistry values. In contrast, the QCISD/6-311++G** ΔE_0 value of Wang and co-workers is -24.71 kcal/mol, and the BSSE correction makes the value too positive, -22.44 kcal/mol.⁴¹ Our results show that there is less BSSE with the double- ζ basis set as the cluster systems become larger, a result that makes intuitive sense. The larger triple- ζ basis set used with the DFT methods has basically eliminated the BSSE, relative to the uncertainty in the experimental values and the accuracy of the high level model chemistry results.

Examining the enthalpic values in Table 1, model chemistry and DFT/aug-cc-pVTZ ΔH°_{298} values are in excellent agreement with each other and with the available experimental information. Pudzianowski reports a MP2/6-311++G(d,p) value of -27.1 kcal/mol for the enthalpy of reaction for an ammonia molecule forming a hydrogen bond with an ammonium ion.³⁹ Our results are similar to those reported by Wang and co-workers using B3LYP/6-31G* and MP2/6-31+G* methodology.⁴¹ The model chemistries' standard deviations from the two experiments are in the range of 0.22–1.40 kcal/mol for enthalpies and 0.65–2.57 kcal/mol for free energies, which compare favorably with the standard deviation of the two experiments to each other, which are 1.09 and 1.02 kcal/mol for enthalpies and free energies, respectively.

The values in Table 2, for complexes of the ammonium cation with water, show excellent agreement with the enthalpies of reaction to form the successive clusters. Results for free energies of reactions are not as good, and in particular addition of a fourth water molecule to the $\text{NH}_4^+(\text{H}_2\text{O})_3$ cluster is predicted by the CBS methods to be about as favorable as addition of the third water molecule to the $\text{NH}_4^+(\text{H}_2\text{O})_2$ cluster, a counterintuitive result that disagrees with experiment. The CBS-QB3 estimate is 1.3 kcal/mol more negative than the low range of the experimental determination, whereas the G2 and G3 results are within 0.5 kcal/mol of the low range of experimental uncertainty. The DFT results using the aug-cc-pVTZ basis set have the correct trend and are all within 1.5 kcal/mol of one of the experimental values. Table 2 shows that the agreement between the two experimental enthalpy determinations is not particularly good, with a standard deviation of 3.02 kcal/mol. Jiang and co-workers report values of ΔH and ΔG that are within 1 kcal/mol of experiment for MP2/6-31+G* calculations with frequencies scaled by 0.969. They also report that B3LYP/6-31+G* calculations with frequencies scaled by 0.973 are not as accurate as the MP2 results.⁴⁵ Tarakeshwar, Kim, and co-workers obtained very good agreement with experiment using MP2/aug-

cc-pVDZ methods and including half the BSSE correction.⁴⁹ It is notable that DFT methods, which are generally thought to behave poorly in predicting weak intermolecular interactions, work well for these strong hydrogen bonds. Although the small 6-31G* basis set is fine for geometries, the much larger aug-cc-pVTZ basis set is essential for capturing the energetics. Given the importance of the formation of $\text{NH}_4^+(\text{H}_2\text{O})_n$ clusters in the atmosphere, outlined in the next section, and the uncertainty between the two experiments, this system should be reexamined with state-of-the-art experimental methods.

Atmospheric Implications. Ions in the atmosphere, which are commonly thought to be present in concentrations of 100–1000 ions/cm³, form clusters through ion–molecule reactions and recombination processes.⁵³ Small ions, besides conducting electricity during thunderstorms, control processes that lead to aerosol formation.^{54–57} A recent experimental study has focused on cycles involving the hydronium and ammonium cations.⁵³ Small ions in the troposphere have lifetimes on the order of hundreds of seconds, and Parks and Luts have studied the effects of certain pollutants on the mobility spectrum of ions that are 1 s old.⁵³ There is much uncertainty regarding the actual concentrations of trace gases, but at the concentrations considered as average values, a combination of experimental and simulation results predicts that the dominant ions existing after one second are $\text{NH}_4^+(\text{H}_2\text{O})_n(\text{NH}_3)_m$ and $\text{H}_3\text{O}^+(\text{H}_2\text{O})_n$.⁵³ Our calculations can shed some insight onto cluster pathways. Table 3 lists the key thermodynamic information for the most important reactions at an agricultural site in the Coastal Plain region of North Carolina.⁵⁸ Measurements made at this site in Clinton, NC, over a year's time reveal average concentrations of 5.32 and 1.84 $\mu\text{g}/\text{m}^3$ for NH_3 and NH_4^+ , respectively. In Clinton, the ammonium cation is the limiting reagent. This is not always the case, as the amount of NH_4^+ can exceed that of NH_3 , so that NH_3 will be the limiting reagent in other agricultural areas. Converting the values at the Clinton, NC, site to concentrations yields values of $[\text{NH}_3]$ of approximately 3.12×10^{-10} M, or 1.88×10^{11} NH_3/cm^3 , and $[\text{NH}_4^+]$ of approximately 1.02×10^{-10} M, or 6.14×10^{10} $\text{NH}_4^+/\text{cm}^3$.

Using the G3 numbers for ΔG° of -18.09 kcal/mol, $K_c = RTK_p = 4.45 \times 10^{14}$, and the reaction of NH_3 and NH_4^+ to make $\text{NH}_4^+(\text{NH}_3)$ produces a concentration of the $\text{NH}_4^+(\text{NH}_3)$ complex of 1.02×10^{-10} M, or 6.14×10^{10} $\text{NH}_4^+(\text{NH}_3)/\text{cm}^3$. Most of the ammonium ion will be complexed with ammonia in the atmosphere above this agricultural site, as either $\text{NH}_4^+(\text{NH}_3)$ or $\text{NH}_4^+(\text{NH}_3)_2$. The actual situation is more complicated, however, because of the presence of water.

Even though ammonia binds to the ammonium cation better than water does,⁵⁹ the high concentration of water in the atmosphere drives the mass action effect to produce fully hydrated ammonium cation clusters. Table 3 lists the concentrations of the product ions from each reaction and shows that the final concentration of $\text{NH}_4^+(\text{H}_2\text{O})_4$ is 3×10^{-10} M, or 2×10^{11} clusters/cm³. The concentration of the ammonium cation is reduced to 3×10^{-19} M, or 191 ions/cm³. The combination of negative free energies and high concentration of water means that most of the $\text{NH}_4^+(\text{NH}_3)$, $\text{NH}_4^+(\text{NH}_3)_2$, and $\text{NH}_4^+(\text{H}_2\text{O})$ clusters will be converted to $\text{NH}_4^+(\text{NH}_3)(\text{H}_2\text{O})_3$, $\text{NH}_4^+(\text{NH}_3)_2(\text{H}_2\text{O})_2$, and $\text{NH}_4^+(\text{H}_2\text{O})_4$ clusters.

As displayed in Tables 2 and 3, the G3 values for ΔG° for formation of $\text{NH}_4^+(\text{H}_2\text{O})_n$ are -14.3 , -8.9 , -6.2 , and -5.4 kcal/mol for $n = 1$ –4 waters. An important difference between these two reactions is that there is much more water in the atmosphere than ammonia, and on a saturated day we would expect the concentration of water vapor to be 0.00180224 M.²⁸ Table 3

shows that these values of ΔG° lead to predicted concentrations of hydrated ammonium ion clusters of approximately 10^6 , 10^8 , 10^8 , and 10^{11} clusters/cm³. The important point is that virtually all of the NH_4^+ ion that is available will be complexed with either an ammonia or water molecule, in this case making approximately 10^{11} clusters/cm³. Because the concentration of water vapor is much greater than the concentration of every ion cluster, all of the NH_4^+ ions will be complexed with three waters and an ammonia molecule at the very least. We would expect that, at this site, the final ions formed on the basis of the analysis presented here are $\text{NH}_4^+(\text{H}_2\text{O})_4$, $\text{NH}_4^+(\text{NH}_3)(\text{H}_2\text{O})_3$, and $\text{NH}_4^+(\text{NH}_3)_2(\text{H}_2\text{O})_2$, with a total concentration of 10^{11} clusters/cm³. We have not calculated the free energy for the formation of the $\text{NH}_4^+(\text{H}_2\text{O})_5$ cluster, and depending on the actual value this would reduce the amount of $\text{NH}_4^+(\text{H}_2\text{O})_4$, $\text{NH}_4^+(\text{NH}_3)(\text{H}_2\text{O})_3$, and $\text{NH}_4^+(\text{NH}_3)_2(\text{H}_2\text{O})_2$ clusters in the atmosphere but not change the number of hydrated ammonium ions. It may be that higher order clusters of ammonia are not abundant, given that the free energy for formation of an ammonium ion cluster by addition of a fifth water or ammonia to the previous cluster was predicted to be around zero,⁴⁵ and addition of a sixth ammonia was positive by approximately 6 kcal/mol.⁴¹

We have previously published work where we examined the ability of the model chemistry methods to predict the thermodynamics of addition of up to four water molecules to the H_3O^+ and OH^- ions.³¹ For the addition of one, two, and three water molecules to the H_3O^+ cation, the standard free energy of reaction at 298.15 K is approximately -26 , -14 , and -10 kcal/mol. Similarly, for the addition of one to four water molecules to the OH^- anion, the free energies are about -19 , -10 , -8 , and -6 kcal/mol. The number of hydrated hydronium and hydroxide complexes will be limited only by the initial number of ions.

Because the free energies for hydration of ions are quite negative, these ions should be effective nucleation sites, lending support to the idea of ions being effective cloud condensation nuclei. Any ion present in the atmosphere will have a negative free energy for complexation with water, and because the concentration of water is relatively high, we predict that virtually all ions are complexed with waters in the atmosphere. The degree of complexation will depend on the free energy of each successive addition of water to the ion. What is unanswered at present is how big the ion clusters can grow. We are currently studying the thermodynamics for formation of larger hydrated ions in our laboratory to gain insight into this question.

Conclusion

The G2, G3, CBS-QB3, and CBS-APNO models and the B3LYP, B3P86, mPW1PW, and PBE1PBE DFT methods have been used to calculate ΔH° and ΔG° values for ionic clusters of the ammonium ion complexed with water and ammonia. Agreement of the model chemistry predictions with the experimental values for ΔH° and ΔG° for formation of $\text{NH}_4^+(\text{NH}_3)_n$ clusters is excellent, with slightly less agreement between experiment and theory for formation of the $\text{NH}_4^+(\text{H}_2\text{O})_n$ clusters. The standard deviation between the two sets of experimental enthalpies is three kcal/mol and we suggest that this atmospherically important cluster reaction be reinvestigated with state-of-the-art experimental methods. The four DFT methods yield very good agreement with experiment and the model chemistry methods when using the aug-cc-pVTZ basis set for energetic calculations and the 6-31G* basis set for geometries and frequencies. At a particular agricultural site in the Southeastern

United States, the concentration of the NH_4^+ ion is $1.84 \mu\text{g}/\text{m}^3$ and the concentration of ammonia is $5.32 \mu\text{g}/\text{m}^3$.⁵⁸ We predict that the total concentration of fully saturated ammonia clusters, $\text{NH}_4^+(\text{H}_2\text{O})_4$, $\text{NH}_4^+(\text{NH}_3)(\text{H}_2\text{O})_3$, and $\text{NH}_4^+(\text{NH}_3)_2(\text{H}_2\text{O})_2$, is on the order of 10^{11} clusters/ cm^3 at this agricultural site. The values for ΔG° are quite negative for addition of 1–4 ammonias or 1–4 waters to the NH_4^+ ion, as are the ΔG° values for addition of 1–3 waters to the H_3O^+ ion and 1–4 waters to the OH^- anion.³¹ The combination of very large equilibrium constants combined with the large relative abundance of water in the atmosphere lead to the prediction that all ions in the lower troposphere will be saturated with at least one complete first hydration shell of water molecules. This study supports the idea of ions being effective cloud condensation nuclei, as any ion present in the atmosphere will have a negative free energy for complexation with water. The extent of complexation will depend on the free energy of each successive addition of water to the ion, and we are currently studying the thermodynamics for formation of large hydrated ions in our laboratory.

Acknowledgment is made to the donors of the Petroleum Research Fund, administered by the American Chemical Society, to Research Corporation, to the Dreyfus Foundation, and to Hamilton College for support of this work. This project was supported in part by NSF grant CHE-0116435 as part of the MERCURY supercomputer consortium (<http://mars.hamilton.edu>). F.C.P. acknowledges support from the Zlinkoff fund, ACS/PRF, and the Ferguson-Seely fund. M.E.D. acknowledges support from ACS/PRF and Research Corporation. We thank Emma Pokon for making preliminary calculations, and Matthew Liptak and Karl Kirschner for insightful comments.

Supporting Information Available: The geometries of all stationary points and absolute energies in hartrees at each level of theory. This material is free of charge via the Internet at <http://pubs.acs.org>.

References and Notes

- (1) Curtiss, L. A.; Raghavachari, K.; Trucks, G. W.; Pople, J. A. *J. Chem. Phys.* **1991**, *94*, 7221.
- (2) Curtiss, L. A.; Raghavachari, K.; Redfern, P. C.; Rassolov, V.; Pople, J. A. *J. Chem. Phys.* **1998**, *109*, 7764.
- (3) Montgomery, J. A.; Frisch, M. J.; Ochterski, J. W.; Petersson, G. A. *J. Chem. Phys.* **1999**, *110*, 2822.
- (4) Ochterski, J. W.; Petersson, G. A.; Montgomery, J. A. *J. Chem. Phys.* **1996**, *104*, 2598.
- (5) Petersson, G. A.; Malick, D. K.; Wilson, W. G.; Ochterski, J. W.; Montgomery, J. A.; Frisch, M. J. *J. Chem. Phys.* **1998**, *109*, 10570.
- (6) Xantheas, S. S. *J. Chem. Phys.* **1996**, *104*, 8821.
- (7) *Negative Ion Energetics Data*; Bartmess, J. E., Ed.; National Institute of Standards and Technology: Gaithersburg, MD, 2000; Vol. <http://webbook.nist.gov>.
- (8) Liptak, M. D.; Shields, G. C. *Int. J. Quantum Chem.*, in press.
- (9) Pokon, E. K.; Liptak, M. D.; Feldgus, S.; Shields, G. C. *J. Phys. Chem. A* **2001**, *105*, 10483.
- (10) Pople, J. A.; Head-Gordon, M.; Fox, D. J.; Raghavachari, K.; Curtiss, L. A. *J. Chem. Phys.* **1989**, *90*, 5622.
- (11) Curtiss, L. A.; Jones, C.; Trucks, G. W.; Raghavachari, K.; Pople, J. A. *J. Chem. Phys.* **1990**, *93*, 2537.
- (12) Curtiss, L. A.; Raghavachari, K.; Pople, J. A. *Chem. Phys. Lett.* **1993**, *214*, 183.
- (13) Curtiss, L. A.; Raghavachari, K.; Redfern, P. C.; Pople, J. A. *J. Chem. Phys.* **1997**, *106*, 1063.
- (14) Curtiss, L. A.; Redfern, P. C.; Raghavachari, K.; Pople, J. A. *J. Chem. Phys.* **1998**, *109*, 42.
- (15) Curtiss, L. A.; Raghavachari, K.; Redfern, P. C.; Kedziora, G. S.; Pople, J. A. *J. Phys. Chem. A* **2001**, *105*, 227.
- (16) Denis, P. A.; Ventura, O. N. *Int. J. Quantum Chem.* **2000**, *80*, 439.
- (17) Jursic, B. S. *THEOCHEM* **2000**, *499*, 91.
- (18) Jursic, B. S. *THEOCHEM* **2000**, *499*, 137.
- (19) Jursic, B. S. *THEOCHEM* **2000**, *499*, 223.
- (20) Jursic, B. S. *THEOCHEM* **2000**, *498*, 123.
- (21) Ochterski, J. W.; Petersson, G. A.; Wiberg, K. B. *J. Am. Chem. Soc.* **1995**, *117*, 11299.
- (22) Zhang, Y.; Zeng, X. R.; You, X. Z. *J. Chem. Phys.* **2000**, *113*, 7731.
- (23) Cramer, C. J. *Essentials of Computational Chemistry: Theories and Models*, 2nd ed.; John Wiley & Sons: New York, 2004.
- (24) Toth, A. M.; Liptak, M. D.; Phillips, D. L.; Shields, G. C. *J. Chem. Phys.* **2001**, *114*, 4595.
- (25) Liptak, M. D.; Shields, G. C. *Int. J. Quantum Chem.* **2001**, *85*, 727.
- (26) Liptak, M. D.; Shields, G. C. *J. Am. Chem. Soc.* **2001**, *123*, 7314.
- (27) Liptak, M. D.; Gross, K. C.; Seybold, P. G.; Feldgus, S.; Shields, G. C. *J. Am. Chem. Soc.* **2002**, *124*, 6421.
- (28) Dunn, M. E.; Pokon, E. K.; Shields, G. C. *J. Am. Chem. Soc.* **2004**, *126*, 2647.
- (29) Dunn, M. E.; Pokon, E. K.; Shields, G. C. *Int. J. Quantum Chem.* **2004**, *100*, 1065.
- (30) Day, M. B.; Kirschner, K. N.; Shields, G. C. *Int. J. Quantum Chem.* **2005**, *102*, 565.
- (31) Pickard IV, F. C.; Pokon, E. K.; Liptak, M. D.; Shields, G. C. *J. Chem. Phys.* **2005**, 024302.
- (32) Becke, A. D. *Phys. Rev. A* **1988**, *38*, 3098.
- (33) Lee, C. T.; Yang, W. T.; Parr, R. G. *Phys. Rev. B* **1988**, *37*, 785.
- (34) Becke, A. D. *J. Chem. Phys.* **1993**, *98*, 5648.
- (35) Adamo, C.; Barone, V. *Chem. Phys. Lett.* **1997**, *274*, 242.
- (36) Perdew, J. P.; Burke, K.; Ernzerhof, M. *Phys. Rev. Lett.* **1996**, *77*, 3865.
- (37) Frisch, M. J.; Trucks, G. W.; Schlegel, H. B.; Scuseria, G. E.; Robb, M. A.; Cheeseman, J. R.; Montgomery, J. A.; Vreven, T.; Kudin, K. N.; Burant, J. C.; Millam, J. M.; Iyengar, S. S.; Tomasi, J.; Barone, V.; Mennucci, B.; Cossi, M.; Scalmani, G.; Rega, N.; Petersson, G. A.; Nakatsuji, H.; Hada, M.; Ehara, M.; Toyota, K.; Fukuda, R.; Hasegawa, J.; Ishida, M.; Nakajima, T.; Honda, Y.; Kitao, O.; Nakai, H.; Klene, M.; Li, X.; Knox, J. E.; Hratchian, H. P.; Cross, J. B.; Adamo, C.; Jaramillo, J.; Gomperts, R.; Stratmann, R. E.; Yazyev, O.; Austin, A. J.; Cammi, R.; Pomelli, C.; Ochterski, J. W.; Ayala, P. Y.; Morokuma, K.; Voth, G. A.; Salvador, P.; Dannenberg, J. J.; Zakrzewski, V. G.; Dapprich, S.; Daniels, A. D.; Strain, M. C.; Farkas, O.; Malick, D. K.; Rabuck, A. D.; Raghavachari, K.; Foresman, J. B.; Ortiz, J. V.; Cui, Q.; Baboul, A. G.; Clifford, S.; Cioslowski, J.; Stefanov, B. B.; Liu, G.; Liashenko, A.; Piskorz, P.; Komaromi, I.; Martin, R. L.; Fox, D. J.; Keith, T.; Al-Laham, M. A.; Peng, C. Y.; Nanayakkara, A.; Challacombe, M.; Gill, P. M. W.; Johnson, B.; Chen, W.; Wong, M. W.; Gonzalez, C.; Pople, J. A. *Gaussian 03*, revision B.02; Gaussian, Inc.: Pittsburgh, PA, 2003.
- (38) Hirao, K.; Fujikawa, T.; Konishi, H.; Yamabe, S. *Chem. Phys. Lett.* **1984**, *104*, 184.
- (39) Pudziaowski, A. T. *J. Chem. Phys.* **1995**, *102*, 8029.
- (40) Park, J. K. *J. Phys. Chem. A* **2000**, *104*, 5093.
- (41) Wang, B.-C.; Chang, J.-C.; Jiang, J.-C.; Lin, S.-H. *Chem. Phys.* **2002**, *276*, 93.
- (42) Rossmeier, T.; Reil, M.; Korber, N. *Inorg. Chem.* **2004**, *43*, 2206.
- (43) Wang, Y.-S.; Chang, H.-C.; Jiang, J.-C.; Lin, S. H.; Lee, Y. T.; Chang, H.-C. *J. Am. Chem. Soc.* **1998**, *120*, 8777.
- (44) Chang, H.-C.; Wang, Y.-S.; Lee, Y. T.; Chang, U.-C. *Int. J. Mass Spectrom.* **1998**, *179/180*, 91.
- (45) Jiang, J. C.; Chang, H. C.; Lee, Y. T.; Lin, S. H. *J. Phys. Chem. A* **1999**, *103*, 3123.
- (46) Chang, T.-M.; Dang, L. X. *J. Chem. Phys.* **2003**, *118*, 8813.
- (47) Nakai, H.; Goto, T.; Okada, Y.; Orii, T.; Takeuchi, K.; Ichihashi, M.; Kondou, T. *J. Chem. Phys.* **2000**, *112*, 7409.
- (48) Fox, B. S.; Beyer, M. K.; Bondybey, V. E. *J. Phys. Chem. A* **2001**, *105*, 6386.
- (49) Lee, H. M.; Tarakeswar, P.; Park, J.; Kolaski, M. R.; Yoon, Y. J.; Yi, H.-B.; Kim, W. Y.; Kim, K. S. *J. Phys. Chem. A* **2004**, *108*, 2949.
- (50) Tang, I. N.; Castleman, A. W. *J. Chem. Phys.* **1975**, *62*, 4576.
- (51) Payzant, J. D.; Cunningham, A. J.; Kebabian, P. *Can. J. Chem.* **1973**, *51*, 3242.
- (52) Meot-Ner (Mautner), M.; Speller, C. V. *J. Phys. Chem.* **1986**, *90*, 6616.
- (53) Parts, T.-E.; Luts, A. *Atmos. Environ.* **2004**, *38*, 1283.
- (54) Vaida, V.; Kjaergaard, H. G.; Feierabend, K. J. *Int. Rev. Phys. Chem.* **2003**, *22*, 203.
- (55) Laakso, L.; Makela, J. M.; Pirjola, L.; Kulmala, M. *Journal of Geophys. Res.—Atmos.* **2002**, *107*, 4427.
- (56) MacTaylor, R. S.; Castleman, A. W. *J. Atmos. Chem.* **2000**, *36*, 23.
- (57) Yu, F.; Turco, R. P. *J. Geophys. Res.—Atmos.* **2001**, *106*, 4797.
- (58) Walker, J. T.; Whittall, D. R.; Robarge, W.; Paerl, H. W. *Atmos. Environ.* **2004**, *38*, 1235.
- (59) Galera, S.; Lluich, J. M.; Oliva, A.; Bertran, J. *THEOCHEM* **1988**, *163*, 101.